AGU PUBLICATIONS

Radio Science

RESEARCH ARTICLE

10.1002/2017RS006389

Key Points:

- The modified cross ambiguity function (MCAF) method can be used to reduce the computational cost in the TDOA/FDOA joint estimation
- The idea of signal segmentation is proposed to solve the problem of code length variation caused by the Doppler effect
- The long-time accumulation (LTA) method can be used to concentrate the signal energy and improve the accuracy of the estimated TDOA/FDOA

Correspondence to:
Y. Zhang,
zyx@xmu.edu.cn

Citation:
Wu, R., Zhang, Y., Huang, Y., Xiong, J., & Deng, Z. (2018). A novel long-time accumulation method for double-satellite TDOA/FDOA interference localization. *Radio Science*, *53*, 129–142. https://doi.org/10.1002/2017RS006389

Received 1 JUN 2017
Accepted 24 DEC 2017
Accepted article online 3 JAN 2018
Published online 31 JAN 2018

A Novel Long-Time Accumulation Method for Double-Satellite TDOA/FDOA Interference Localization

Risheng Wu[1], Yixiong Zhang[1], Yanan Huang[1], Jinyi Xiong[2], and Zhenmiao Deng[1]

[1]School of Information Science and Engineering, Xiamen University, Xiamen, China, [2]Key Lab of Blind Signal Processing, Chengdu, China

Abstract In double-satellite interference localization system, the position of the interference source is computed by estimating the time difference of arrival (TDOA) and the frequency difference of arrival (FDOA) between the signals retransmitted by two satellites. The traditional cross ambiguity function (CAF)-based TDOA/FDOA estimation method requires the constant TDOA/FDOA between the two received signals, which can be satisfied only when the signal length is short. Therefore, the CAF estimation method cannot be applied in long-time accumulation (LTA). To solve this problem, a novel LTA method is proposed based on signal segmentation. In the proposed method, the two received signals are first divided into several short signal segments. Subsequently, the TDOA, the initial FDOA, and the FDOA change rate of each signal segment are estimated by a modified CAF method. After compensating the FDOA difference between the signal segments, the results are spliced again to form a complete signal without FDOA variation. Consequently, the signal energy can be concentrated and the estimation accuracy of FDOA can be improved. Experimental results of real data demonstrate that greater signal-to-noise ratio (SNR) gain is achieved by the proposed method, compared to the traditional CAF-based method.

1. Introduction

Nowadays, satellite communication is widely used in military, civil, and commercial fields. However, the interference events of communication satellites constantly happen on a global scale (Coleman, 2015; Dempster & Cetin, 2016; Haworth, 2000; Isoz et al., 2014). Ordinary malicious interference destroys the normal satellite communication services, while the interference in military confrontation may endanger the national security. For this reason, research on satellite interference localization is of great importance to maintain the normal services of satellite communication.

There are some typical techniques used for interference localization, such as the received signal strength (RSS) (Malaney, 2007; Thompson, 2015), angle of arrival (AOA) (Dempster, 2006; Trinkle & Gray, 2002), time difference of arrival (TDOA) (Kay, 1993), and frequency difference of arrival (FDOA) (Haworth et al., 1997; Musicki & Koch, 2008). Most interference localization systems rely on either one or multiple techniques to implement interference localization. The main advantage of the RSS technique is its low implementation complexity, but its performance degrades with increased distance. AOA technique can be applied for any signal bandwidth, but the performance of AOA technique is quite poor in cases of multipath and larger distance. Besides, the implementation complexity of AOA technique is high, and it requires calibration for antenna array (Xu et al., 2010). Compared to AOA technique, the advantage of TDOA technique is that its accuracy does not degrade with distance, but it may suffer from poor performance for narrowband signals (Kay, 1993). On the other hand, FDOA technique requires narrowband signals. Thus, the TDOA/FDOA hybrid method can be suitable for a much wider range of sources (Musicki et al., 2010). In addition, the TDOA/FDOA method can provide more accurate interference localization than other methods.

In single-satellite localization systems, although the interferometery based on AOA can be used to obtain the phase estimation, it still should be combined with TDOA to locate the interference (Smith & Steffes, 1990). A key technique in single-satellite localization systems is the FDOA method (Ho et al., 2013), which locates the interference by calculating the variation FDOA or frequency of arrival (FOA) (Kalantari et al., 2016). However, it needs to solve many location-related equations. The correlation algorithm proposed in Michael (2015) relies on the power of a satellite signal, and the challenge lies in the correlation approach since the measurements are typically not performed at exactly the same time. Compared to single-satellite localization system, the double-satellite localization system can provides a more reliable location performance because two or more localization techniques are adopted.

TDOA/FDOA estimations are generally adopted in double-satellite interference localization systems, such as the TLS Model 2000 system in the United States and the SatID system in Europe (Kimball, 2011; Kallan & Baykal, 2014). In the literatures, there are several TDOA/FDOA estimation methods. For example, the maximum likelihood (ML) (Knapp & Carter, 1977; Stein, 1993; Wax, 1982) estimator requires long observation and high signal-to-noise ratio (SNR) to ensure the estimation accuracy. The expectation maximization (EM) algorithm is able to estimate the TDOA/FDOA parameters in cases where the source signal and the noise spectra are unknown in advance (Dempster et al., 1977). However, the iterative procedure (Belanger, 1993) contained in the EM algorithm is computationally intensive. The adaptive digital delay-look discriminator (ADDLD) method and the least mean square algorithm for time delay estimation (LMSTDE) method are evaluated in Youn and Ahmed (1984). Compared to the LMSTDE method, the main advantage of the ADDLD method is its computational simplicity, the constraint conditions of which, however, limit its application; more details can be seen in Youn and Ahmed (1984). The classical method of parameter estimation used in double-satellite interference localization system is the crossing ambiguity function (CAF) algorithm based on correlation principle (Guo et al., 2016; Ho & Xu, 2004; Hu et al., 2016; Zhang & Zhang, 2011). The CAF algorithm is able to locate the interference position for signals with different modulations and bandwidths, without affecting the normal function of satellite communications.

The CAF algorithm estimates the TDOA and FDOA through a two-dimensional search; thus, its computational cost is high. Besides, it requires the TDOA and FDOA of the two received signals to be constant. When the SNR of the received signal is relatively low, long-time accumulation (LTA) is needed to concentrate the signal energy (Yao et al., 2005). However, as the motions of the two satellites are generally different, the SNR after the CAF operation cannot be improved by LTA without effectively compensating for the motion differences of the two satellites.

In this paper, we propose a long-time accumulation method for TDOA/FDOA estimation in the double-satellite interference localization system. First, the input signals are divided into several short segments, of which the TDOAs can be considered to be constant. Then, for each signal segment, the TDOA, the initial FDOA, and the FDOA change rate are estimated. After FDOA compensation, the correlation results are spliced again to form a complete signal without FDOA variation. As a result, the signal energy is concentrated and the FDOA estimation accuracy can be improved. When estimating the TDOA/FDOA parameters, a modified CAF algorithm based on the second-order-statistics (MCAF-SOS) is used to reduce the computational cost. Experimental results of real data demonstrate the effectiveness of the proposed LTA method.

The rest of this paper is organized as follows. In section 2, the signal model of the double-satellite localization system is presented, then we review the CAF-based TDOA/FDOA estimation methods and analyze their performances. In section 3, we first discuss the problem to be solved in LTA. After introducing the idea of signal segmentation, the LTA method is proposed in detail. Experimental results on real data are analyzed in section 4. Finally, the conclusion is given in section 5.

2. Model of Double-Satellite Localization and Joint Parameter Estimation Algorithm

2.1. Model of Double-Satellite Localization System

2.1.1. Principle of Double-Satellite Localization System

The double-satellite TDOA/FDOA interference localization system (Mason, 2004) is illustrated in Figure 1. When the interference source transmits interference signal, the main lobe of the signal points to the interfered satellite (or the primary satellite), while the sidelobe may point to the adjacent satellite. In general, it is assumed that the interference signal is narrow band, and both satellites move along similar directions with similar speeds. Two ground stations are used to detect the interference signals retransmitted by the two satellites. As the retransmitted interference signals arrive at the ground stations with different propagation delays, there is a time difference of arrival, that is, TDOA, between the two received signals. In addition, the distance between the satellite and the Earth does not keep constant but drifts in their orbits, because the synchronous satellite in the orbit is affected by a variety of photodynamic forces, such as lunar attraction, aerodynamic force of the upper atmosphere, and the Earth shape of the nonspherical additional gravity. Therefore, the Doppler frequency shifts of the two received signals are different, and there exists a frequency difference

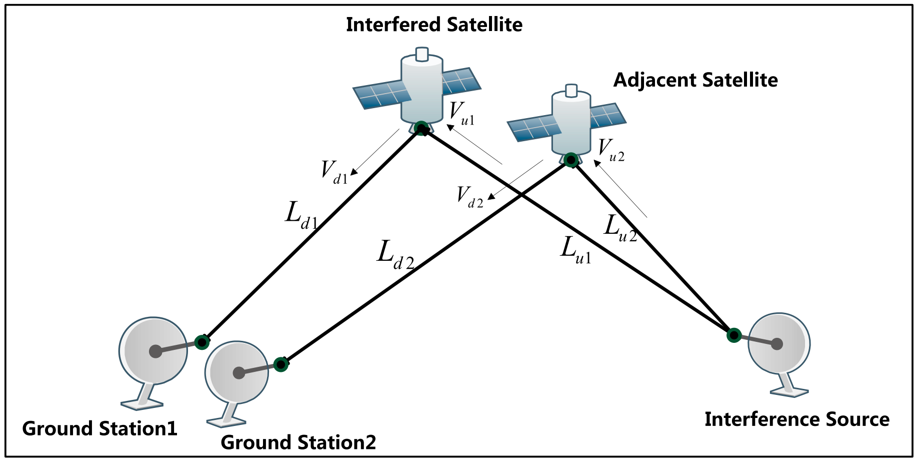

Figure 1. Schematic of the double-satellite interference localization system.

of arrival, that is, FDOA, between the received signals. Given that the positions of the two satellites relative to ground stations are known, TDOA over the two different paths isolates the possible interference location to a one-dimensional curve on the Earth's surface and FDOA determines another curve similarly. As a result, we can compute the interference position by determining the intersection of the two curves. In fact, the location of the interference should be affected by many factors, such as the satellite positions/velocities, the frequency of the oscillator in the satellites, and the estimated TDOA/FDOA values. Meanwhile, before solving the location-related equations, the TDOA/FDOA need to be calibrated by a reference station with known position. In this paper, we mainly focus on the methods of improving the accuracy of the estimated TDOA/FDOA before calibration.

As shown in Figure 1, the distance between the interference source and the two satellites are denoted by L_{u1} and L_{u2} , respectively. L_{d1} is the distance between the ground station 1 and the interfered satellite, while L_{d2} is the distance between the ground station 2 and the adjacent satellite. The TDOA between the two signals arriving at the ground stations is given by (Deng et al., 2012)

$$\Delta\tau = \frac{L_{u1} + L_{d1}}{c} - \frac{L_{u2} + L_{d2}}{c}, \tag{1}$$

where $c \approx 299{,}792{,}458$ m/s is the speed of electromagnetic wave.

Due to the relative motion between the satellite and the interference source as well as the ground stations, the Doppler frequency shifts of the two received signals are different. Let f_u and f_d be the carrier frequency of the uplink and the downlink signals, respectively. The radial velocities of the two satellites relative to interference source are denoted as V_{u1} and V_{u2} , respectively. V_{d1} is the radial velocity of the interfered satellite relative to ground station 1, and V_{d2} is the radial velocity of the adjacent satellite relative to ground station 2. The FDOA between the two signals arriving at the ground stations can be written as (Wu et al., 2010)

$$\Delta f = \frac{f_u}{c} \cdot \left(V_{u1} - V_{u2}\right) + \frac{f_d}{c} \cdot \left(V_{d1} - V_{d2}\right). \tag{2}$$

2.1.2. Signal Model

Assuming $x(n)$ and $y(n)$ denote the received signals retransmitted by the interfered satellite and adjacent satellite, respectively, the received signal model of the double-satellite interference localization system can be expressed as (Fowler & Hu, 2008)

$$\begin{cases} x(n) = s(n) + w^1(n) \\ y(n) = As(n - D)\exp\left\{j\left[2\pi\Delta f \frac{(n-D)}{f_s} + \phi\right]\right\} + w^2(n), \end{cases} \tag{3}$$

where $n = \{1, 2, 3, \dots, N\}$ and N is the length of the discrete digital sequence. A and $\phi \in (-\pi, \pi]$ denote the involved attenuation factor and constant phase difference, respectively. f_s is the sampling rate, and $s(n)$ is the signal of interference source. D and Δf denote the TDOA and FDOA between the two received signals, respectively. Here the discrete value of TDOA D satisfies that $\Delta\tau \cdot f_s = D$, and the $\Delta\tau$ is continue value of TDOA.

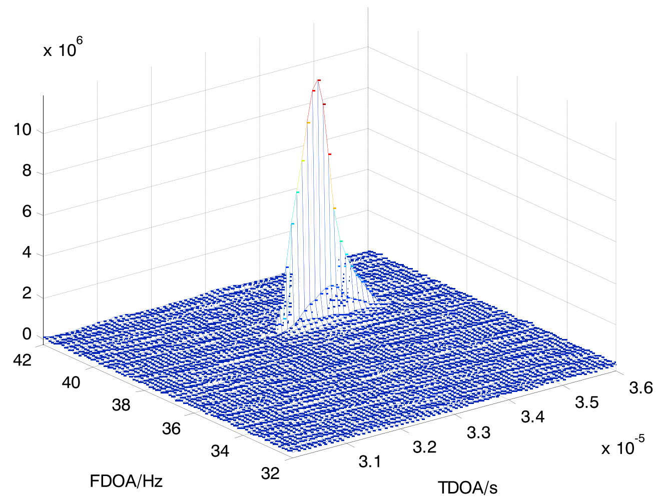

Figure 2. An example of the CAF results.

The additive noise $w^1(n)$ and $w^2(n)$ are both assumed to be stationary, zero mean, temporally white, and normally distributed. Here $w^1(n)$ and $w^2(n)$ are assumed to be uncorrelated with each other and both are independent of the signal. In general, this is a common assumption.

2.2. TDOA/FDOA Joint Estimation Based On CAF

In the double-satellite interference localization system, estimation of TDOA/FDOA is the key to the localization algorithm, and the accuracy of estimated TDOA/FDOA directly affects the positioning performance. In this section, we first review the traditional CAF estimation method first. A low complexity modified CAF (MCAF) method involving fast Fourier transform (FFT) and frequency estimation algorithm is then presented. Finally, the performances of the CAF-based methods are analyzed.

2.2.1. CAF Estimation Algorithm

The CAF based on the second-order-statistics (CAF-SOS) of the two received signals is defined as follows (Dandawate & Giannakis, 1993):

$$\mathrm{CAF}(\tau, f) = \int_0^T x(t)y^*(t+\tau)e^{-j2\pi ft}\mathrm{d}t, \tag{4}$$

where $x(t)$ and $y(t)$ denote the two received signals, respectively, T is the accumulation time. τ and f denote the value of TDOA and FDOA to be searched between the two received signals, respectively. Asterisk denotes the conjugation operation. The function is essentially a correlation operation between $x(t)$ and $y(t+\tau)$. As a result, $x(t)y^*(t+\tau)$ contains second-order statistics (Stein, 1981). Therefore, equation (4) is known as CAF-SOS. It is noted that CAF can also be combined with higher-order statistics (HOS), for example, CAF-based fourth-order-statistics (CAF-FOS) algorithm (Shan et al., 2008). However, the use of CAF-based higher-order-statistics (CAF-HOS) (Shin & Nikias, 1993) is impractical because of large computational cost. For this reason, only CAF-SOS is considered in this paper.

By converting (4) to a discrete sequence, one gets

$$C_{xy}(\tau, f) = \sum_{n=0}^{N-1} x(n)y^*(n+\tau)e^{-j2\pi f\frac{n}{f_s}}, \tag{5}$$

where N is the length of the digital sequence. In CAF-SOS, the TDOA/FDOA can be estimated by maximizing the function over the two parameters, that is, $(\hat{\tau}, \hat{f}) = \max_{\tau,f} C_{xy}(\tau, f)$. An example of the function $C_{xy}(\tau, f)$ with respect to τ and f is shown in Figure 2, from which the estimated results, that is, $\hat{\tau}$ and $\hat{f}$, can be obtained.

2.2.2. Modified CAF Algorithm

The traditional CAF-SOS algorithm requires a two-dimensional search to estimate the TDOA/FDOA parameters. Actually, the search of FDOA can be realized by FFT, which can greatly speed up the estimation process (Lin & Tsui, 2014).

The modified CAF-SOS involving FFT can be represented as follows:

$$S_{xy}(\tau, f) = \mathcal{F}\left\{x(n)y^*(n+\tau)\right\}, \tag{6}$$

where $\mathcal{F}\{\}$ means the FFT operation. Substituting (3) into (6), and assuming the noise is independent of the signal, one obtains

$$S_{xy}(\tau, f) = \mathcal{F}\left\{As(n)s^*(n-D+\tau)\exp\left\{-j\left[2\pi\Delta f\frac{(n-D+\tau)}{f_s}+\phi\right]\right\}\right\}. \tag{7}$$

According to the exponential term $\exp\left\{-j\left[2\pi\Delta f\frac{(n-D+\tau)}{f_s}+\phi\right]\right\}$ in (7), there is a peak value at frequency $\hat{f}_\tau$ in the spectrum $S_{xy}(\tau, f)$. $\hat{f}_\tau$ means the peak position of the spectrum corresponding to τ. When $\tau = D$, $s(n)s^*(n-D+\tau)$ becomes a direct current (DC) signal, and the value of the peak spectrum position at $\hat{f}_D$ is the largest. When $\tau \neq D$, the value of the peak at $\hat{f}_\tau$ is smaller than that of the DC signal, that is, $S_{xy}(\tau, \hat{f}_\tau) \leq S_{xy}(D, \hat{f}_D)$. Therefore, only one-dimensional search along τ is necessary to estimate the TDOA. In addition, to further improve the accuracy of the estimated FDOA, a number of sinusoidal frequency estimation algorithms

(Rife & Vincent, 1970; Tsui, 2004; Xiao et al., 2004) can be used. Specifically, the Rife iterative algorithm (Tsui, 2004) is adopted in this paper due to its stable performance.

2.2.3. Analysis of the CAF-Based Algorithm

Since the signals retransmitted by the interfered satellite and the adjacent satellite contain additive noise, there is a SNR loss in the correlation operation (Stein, 1981). The SNR of the correlation result after FFT, named as accumulated SNR in this paper, can be represented by

$$\mathrm{SNR}_c = \frac{2BT \cdot \mathrm{snr}_1 \cdot \mathrm{snr}_2}{1 + \mathrm{snr}_1 + \mathrm{snr}_2}, \tag{8}$$

where B is the channel bandwidth and T is the accumulation time. snr_1 and snr_2 are the SNRs of received retransmitted signals.

In most cases, the adjacent satellite lies in the sidelobe of the antenna pattern of the interference source, and the SNR of its received signal is very low. To concentrate the signal energy, it is necessary to increase the time bandwidth product BT. In general, the channel bandwidth B is fixed, and therefore, increasing the accumulation time T is a feasible way.

The traditional CAF-SOS algorithm requires a two-dimensional search to estimate the TDOA/FDOA parameters; thus, its computational cost is high. Assuming the search ranges of TDOA and FDOA are R_τ with searching step of d_τ and R_f with searching step of d_f, respectively. The search number of TDOA is $n_\tau = \frac{R_\tau}{d_\tau}$ and that of FDOA is $n_f = \frac{R_f}{d_f}$. Supposing that the length of discrete signal is n_d, the time complexity of a two-dimensional search in CAF-SOS is $O(n_\tau n_f n_d)$, while that of the MCAF method is $O(n_\tau n_d \lg n_d)$. Assuming the sampling rate is f_s, it should satisfy that $n_f = \frac{R_f n_d}{f_s}$ if the CAF-SOS and MCAF have the same estimation precision of FDOA. In general, the MCAF algorithm can greatly speed up the estimation process because $\frac{R_f n_d}{f_s} \gg \lg(n_d)$ is satisfied in general cases. For example, supposing the time length of the signal is 53 s, the sampling rate f_s is 2.5×10^6 Hz. The search range of TDOA is $(75 \sim 90)/f_s$ with step of $1/f_s$, and the search range of FDOA is $(32 \sim 42)/f_s$ with step of 0.1 Hz. The total time cost of the CAF-SOS algorithm in (5) is 5.013 h, while the MCAF-SOS algorithm in (7) only needs 211 s.

3. Proposed Long-Time Accumulation Method

To improve the accuracy of estimated TDOA/FDOA, we propose a novel LTA method based on signal segmentation in this paper. First, the input signals are divided into several short signal segments. Then the TDOA/FDOA is estimated for each segment. After FDOA compensation, the signal segments are spliced to improve the estimation performance.

In this section, the problem in LTA is first analyzed based on the characteristic of TDOA/FDOA. Then the signal segmentation idea of the proposed method is demonstrated. Finally, the algorithm of the proposed LTA method is introduced in detail.

3.1. Problem Description

According to (4), the traditional CAF-SOS method estimates TDOA/FDOA by a two-dimensional search, which requires constant TDOA/FDOA in the accumulation time interval. This assumption can be approximately satisfied for short accumulation time, for example, dozens of seconds. However, for LTA cases, the drifts of TDOA/FDOA in the accumulation time interval (e.g., hundreds of seconds) cannot be ignored anymore (Zhang & Zhang, 2011). Given the location of the interference source and the ground station, we can depict the variation of TDOA/FDOA according to (1) and (2). Examples of TDOA/FDOA variation in 48 h are shown in Figures 3 and 4, respectively.

It is seen that the variations of TDOA/FDOA are sinusoidal with a period of 24 h. When the accumulation time becomes longer, such as hundreds of seconds, TDOA/FDOA cannot be viewed as constants. In general, part of the sine-wave curve can be expanded by the Taylor series. In our experiments, a one-order or second-order Taylor series is enough for the signal with a length of hundreds of seconds.

3.2. The Idea of Signal Segmentation in the Proposed LTA Method

3.2.1. Change of Code Length Caused by the Doppler Effect

In double-satellite interference localization model, the influence of TDOA/FDOA variation is mainly on the code misalignment (Tsui, 2005). However, the traditional CAF-SOS algorithm only considers the influence

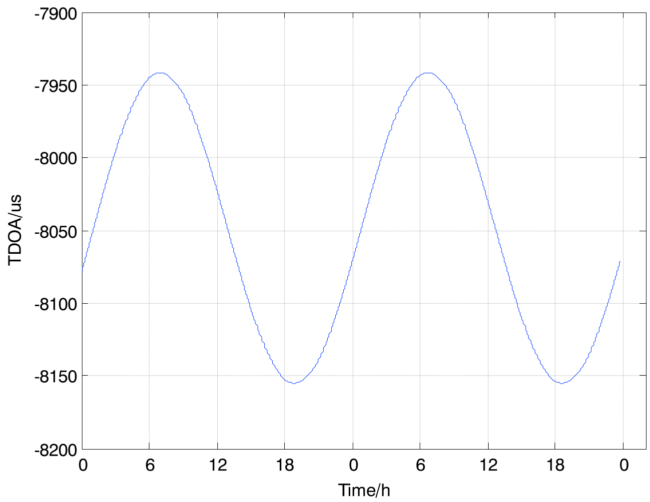

Figure 3. The variation of TDOA in 48 h.

of Doppler effect on the carrier frequency but neglects the Doppler effect on the code length. The change of code length caused by the Doppler effect can be expressed as (Lin & Tsui, 2002),

$$T_{cd} = T_c \frac{f_L}{f_L + f_d}, \tag{9}$$

where T_c is the original code length, T_{cd} is the new code length, f_L is the carrier frequency, and f_d is the Doppler shift.

Since the Doppler shifts of the two received signals are different, the code length of the two signals is slightly different. When accumulating for a long-time, this small error will be accumulated and amplified. As a result, the performance of TDOA/FDOA estimation by the CAF algorithm will decrease due to the code misalignment. This phenomenon will be shown in section 4.1.

3.2.2. Consideration of the Length of Segmentation

In order to avoid accumulating of misaligned code, the input signal is divided into small segments whose length is about dozens of seconds. As the length of the segment is short, the TDOA in each signal segment can be regarded as constant. The first task is to determine the length of the signal segment.

In our method, one principle to determine the segment length is that the variation of TDOA in a segment will not exceed a sampling period. Supposing the TDOA changes at a rate of α, then the segment length T_{seg} should satisfy

$$\alpha \cdot T_{\text{seg}} \le \frac{1}{f_s}, \tag{10}$$

where f_s is the sampling rate. In this manner, the TDOA of each segment can be viewed as a constant, which satisfies one of the conditions of the CAF algorithm. In the implementation stage, the estimated TDOA of a segment can be regarded as the TDOA at the beginning time of the segment.

In fact, at the beginning of TDOA/FDOA estimation, the accurate value of α is not available, and the segment length cannot be calculated by (10). Alternatively, the segment length is initially set to a small value T_x, then we can select the first and the last segment to estimate their coarse TDOAs. Assuming the coarse estimates of the first and the last segment are $\hat{D}_{\text{first}}$ and $\hat{D}_{\text{last}}$, then the change rate of TDOA can be calculated by $\alpha = \frac{\hat{D}_{\text{last}} - \hat{D}_{\text{first}}}{T \cdot f_s}$, where T is the total length of the input signal, that is, the total accumulation time. Finally, the segment length can be calculated by $T_{\text{seg}} = \frac{1}{\alpha \cdot f_s}$, shown in Figure 5.

3.3. Proposed LTA Method

As shown in Figure 4, the variation of FDOA is sinusoidal with a period of 24 h, which can be approximated by a Taylor series. However, for a short segment, the variation of FDOA can be considered to be linear. Accordingly, the phase difference between the two received signals can be expressed as a second-order polynomial.

3.3.1. Refined Signal Model

In the proposed LTA method, the two received signal $x(n)$ and $y(n)$ are divided into short signal segments, that is, $x_i(n)$ and $y_i(n)$, where i $(1 \le i \le I)$ is the index of the segment and I is the total number of segments. Considering the variation of FDOA, the signal model of the proposed method can be refined as

$$\begin{cases} x_i(n) = s_i(n) + w_i^1(n), \\ y_i(n) = A_i s_i(n - D_i) \exp\left\{ j \left[2\pi \Delta f_i \frac{(n - D_i)}{f_s} + \pi k_i \left(\frac{n - D_i}{f_s} \right)^2 + \phi_i \right] \right\} + w_i^2(n), \end{cases} \tag{11}$$

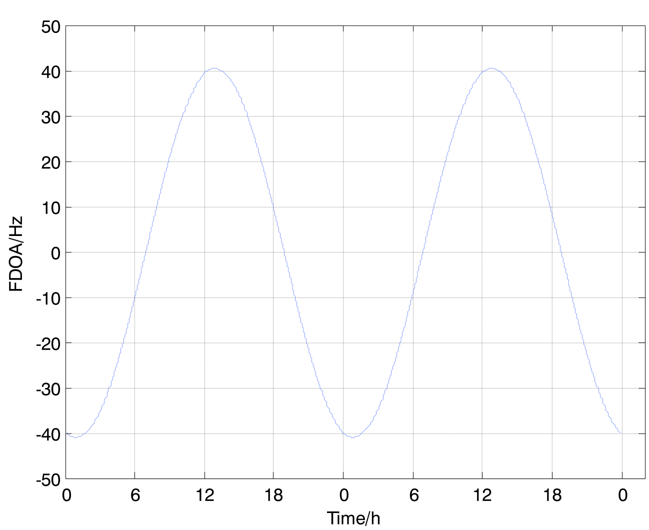

Figure 4. The variation of FDOA in 48 h.

where the subscript "i" means the signal or the parameter of the ith signal segment. $w_i^1(n)$ and $w_i^2(n)$ are the noise terms of the two channels.

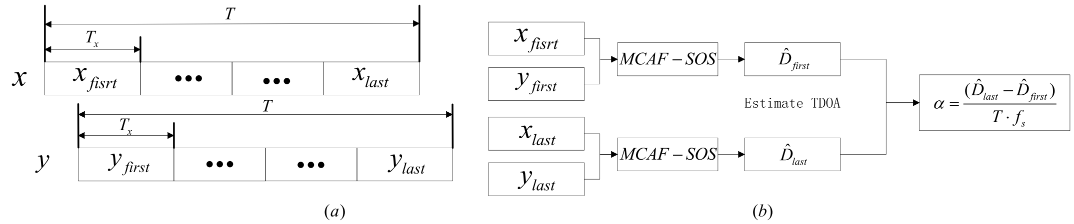

Figure 5. Flow chart of estimation of TDOA change rate.

Δf_i denotes the initial FDOA between the two signal segments, while k_i denotes the change rate of FDOA. As described above, the TDOA between the two signal segments is viewed as a constant and denoted by D_i. A_i and $\phi_i \in (-\pi, \pi]$ denote the attenuation factor and the phase difference between the two received signals, respectively.

3.3.2. Estimation of TDOA and FDOA

From (11), there is a second-order term in FDOA between the two received signal segments; thus, the CAF or MCAF algorithm cannot be applied directly to estimate the TDOA and FDOA. It is known that there are three parameters to be estimated, that is, D_i, Δf_i, and k_i. As stated in the MCAF algorithm, estimation of Δf_i can be implemented by the Rife iterative algorithm. Then the estimation problem can be solved by a two-dimensional search over D_i and k_i. However, the computational cost is large. In the proposed method, a fast approach is adopted.

In the refined signal model, (11), k_i will broaden the main lobe of the spectrum at Δf_i. In other words, k_i mainly affects the estimation accuracy of Δf_i instead of D_i. Therefore, in order to estimate D_i, k_i can be ignored at first. After obtaining the TDOA estimates, the estimation is transformed to a one-dimensional search problem with respect to k_i. The estimation algorithm is described as follows.

First, we estimate TDOA using the MCAF algorithm. Supposing the estimated TDOA is $\hat{D}_i$, then the estimation of k_i can be formulated as

$$S^i_{xy}(\hat{D}_i, \beta, f) = \mathcal{F}\left\{ x_i(n) y_i^*(n + \hat{D}_i) \exp\left[-j\pi\beta \left(\frac{n}{f_s}\right)^2 \right] \right\}, \tag{12}$$

where β is the search value of k_i. Replacing $x_i(n)$ and $y_i(n)$ in (12) with that in (11), one gets

$$S^i_{xy}(\hat{D}_i, \beta, f) = \mathcal{F}\left\{ \begin{array}{l} A_i s_i(n) s_i^*(n - D_i + \hat{D}_i) \exp\left\{ -j\left[2\pi\Delta f_i \frac{(n - D_i + \hat{D}_i)}{f_s} + \phi_i \right] \right\} \\ \times \exp\left\{ -j\pi(\beta + k_i)\left(\frac{n}{f_s}\right)^2 \right\} \end{array} \right\}. \tag{13}$$

Without loss of generality, we can set $\varphi_i = 0$. When $\hat{D}_i = D_i$, (13) is simplified as

$$S^i_{xy}(D_i, \beta, f) = \mathcal{F}\left\{ A_i s_i(n) s_i^*(n) \exp\left\{ -j2\pi\Delta f_i \frac{n}{f_s} \right\} \exp\left\{ -j\pi(\beta + k_i)\left(\frac{n}{f_s}\right)^2 \right\} \right\}. \tag{14}$$

Then k_i and $\Delta\hat{f}_i$ can be estimated by searching the peak of $S^i_{xy}(D_i, \beta, f)$. That is,

$$\{\hat{k}_i, \Delta\hat{f}_i\} = \max_{\beta}\left(S^i_{xy}(D_i, \beta, f) \right). \tag{15}$$

To reduce the time cost of solving k_i, the sequential quadratic programming (SQP) (Spellucci, 1998) algorithm is adopted. Compared to the traditional step-by-step search, SQP algorithm can obtain better estimation precision with much less computational complexity. Note that the SQP algorithm may obtain local optimal solution with some special initial value of k_i. To avoid this, a number of initial values of k_i should be set to obtain the global optimal solution.

3.3.3. FDOA Compensation for LTA

To focus the energy of the total input signal, the FDOA between the two received signals should be compensated for each segment, before splicing the signal segments. After estimating the three parameters, that is, D_i, Δf_i, and k_i, the FDOA diagram is illustrated in Figure 6. The objective of FDOA compensation is to align

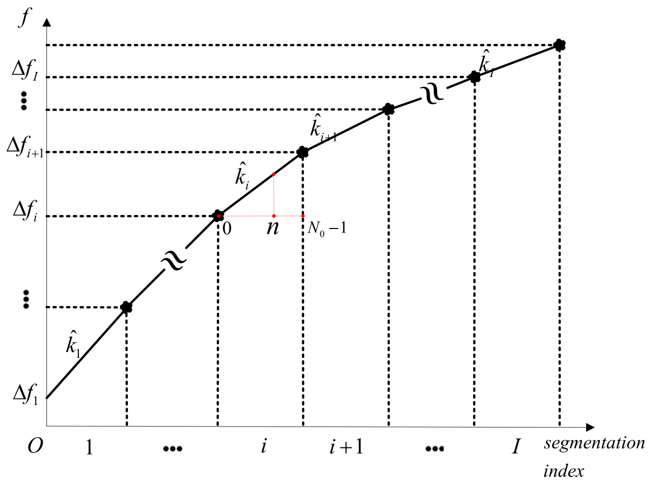

Figure 6. Illustration of FDOA variation for signal segmentations.

the frequency at any time with that of the start point, that is, Δf_1. As seen from Figure 6, the frequency difference between any point in the accumulation interval and the start point can be represented by

$$\Delta \hat{f}_i(n) = (\Delta \hat{f}_i - \Delta \hat{f}_1) + \hat{k}_i \left(\frac{n}{f_s}\right). \tag{16}$$

Therefore, with FDOA compensation, the correlated signal can be expressed as

$$\hat{y}_i(n) = y_i(n + \hat{D}_i) \exp\left\{-j2\pi(\Delta \hat{f}_i - \Delta \hat{f}_1)\left(\frac{n}{f_s}\right)\right\} \exp\left\{-j\pi \hat{k}_i \left(\frac{n}{f_s}\right)^2\right\}. \tag{17}$$

And the correlation result after FDOA compensation is

$$\begin{aligned}\hat{s}^i_{xy}(n) &= x_i(n)\hat{y}^*_i(n)\\ &= x_i(n)y_i^*(n+\hat{D}_i)\exp\left\{-j2\pi(\Delta \hat{f}_i - \Delta \hat{f}_1)\left(\frac{n}{f_s}\right)\right\}\exp\left\{-j\pi \hat{k}_i\left(\frac{n}{f_s}\right)^2\right\}\\ &= s^i_{xy}(n)\exp\left\{-j2\pi(\Delta \hat{f}_i - \Delta \hat{f}_1)\left(\frac{n}{f_s}\right)\right\}\exp\left\{-j\pi \hat{k}_i\left(\frac{n}{f_s}\right)^2\right\},\end{aligned} \tag{18}$$

where $s^i_{xy}(n) = x_i(n)y_i^*(n + \hat{D}_i)$ is the correlation result without FDOA compensation. It can be seen that the correlation and the compensation operation are exchangeable. The FDOA compensation includes two parts, that is, the FDOA variation $\hat{k}_i$ inside the segment and the FDOA difference between the ith segment and the first segment, that is, $\Delta \hat{f}_i - \Delta \hat{f}_1$. Then, the signal segments after correlation are spliced as

$$\hat{s}_{xy}(m) = \left[\hat{s}^1_{xy}(n), \hat{s}^2_{xy}(n), \ldots, \hat{s}^i_{xy}(n), \ldots, \hat{s}^I_{xy}(n)\right], \tag{19}$$

where $m = (0, \ldots, IN_0 - 1)$ is the index of the spliced signal. Finally, the Rife iterative algorithm is applied to $\hat{s}_{xy}(m)$ to estimate Δf_1. Consequently, the accuracy of FDOA can be improved significantly, due to the long-time accumulation operation.

3.3.4. Flow Chart of the Proposed LTA Method

The flow chart of the proposed LTA method is shown in Figure 7. First, the two received signals, $x(n)$ and $y(n)$, are divided into short signal segments, that is, $x_i(n)$ and $y_i(n)$, $i\,(1 \le i \le I)$. The length of the segment is determined by (10). Subsequently, the MCAF-SOS algorithm is performed on each signal segment to estimate the TDOA $\hat{D}_i$. With $\hat{D}_i$, the Rife iterative algorithm and the SQP algorithm are carried out to estimate the initial FDOA and the FDOA variation rate of the segment, denoted by $\Delta \hat{f}_i$ and $\hat{k}_i$, respectively. Then, FDOA compensation as shown in (18) is applied to the correlation result for the segment. Finally, the compensated signal segments are spliced again as a complete signal without FDOA variation. The signal energy can be concentrated due to the long-time accumulation.

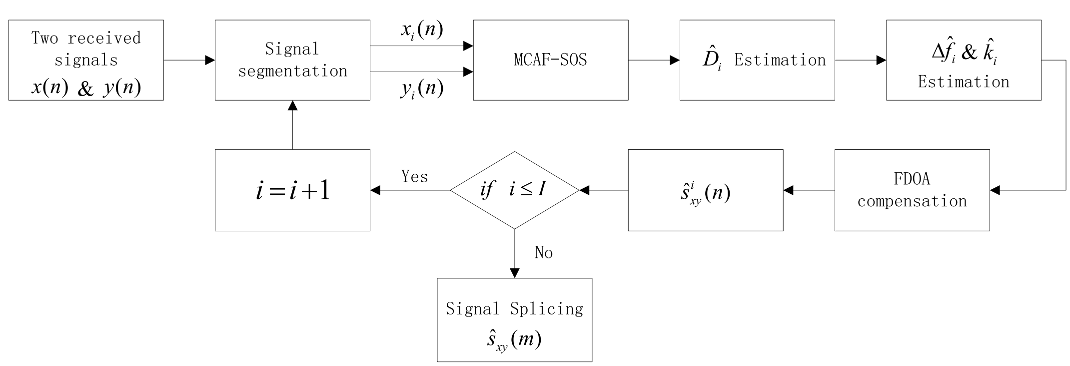

Figure 7. The flow chart of the proposed LTA method.

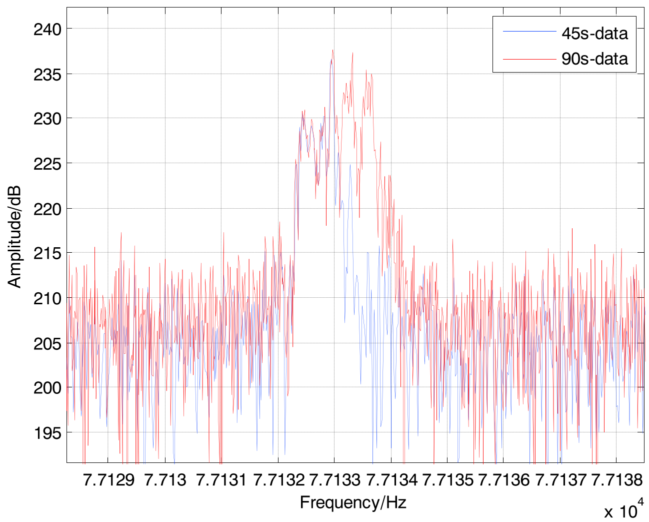

Figure 8. Comparison of spectrum between the 45 s data and the 90 s data.

4. Experimental Results on Real Data

In this section, two sets of real data are used to verify the validity and the effectiveness of the proposed LTA method. For convenience, the two sets of real data are named as DATA1 and DATA2, respectively. Each data set contains two signals retransmitted by two satellites. The sampling rate is 2.5 MHz. The time length of DATA1 is 600 s, while that of DATA2 is 580 s. According to the principle of (10), the segment length of DATA1 is set to 45 s, while the segment length of DATA2 is set to 40 s. Therefore, the number of segments of DATA1 is 13, and that of DATA2 is 14.

In the following experiments, to compute the SNR for real data, the noise power is estimated by averaging the spectrum power outside the signal band. The results without FDOA compensation are first demonstrated, then the compensation results by using the proposed LTA method are analyzed in detail.

4.1. Results Without FDOA Compensation

As discussed in section 3.1, the CAF-based estimation method cannot be used directly in long-time accumulation. To intuitively describe this problem, the MCAF method is performed on the signal with different time length extracted from the test data .

Figure 8 compares the spectrum of the correlation results of DATA1 between the one data segment (45 s data) and the two data segments (i.e., 90 s data). It can be seen that the bandwidth of the two data segments is larger than that of the one data segment, as the FDOA variation is not compensated. This also implies that the FDOA changes with time. The SNR after accumulation (i.e., accumulated SNR) of the one data segment is 33.4811 dB, while that of the two data segments is 31.5172 dB. The fundamental reason of the correlation results shown in Figure 8 is that the FDOA difference between the signal segments is not effectively compensated. Even if the accumulation time is increased, the accumulated SNR decreases.

In addition, the accumulated SNRs of the signals with different accumulation time are shown in Table 1. It is obvious that the SNR decreases when the segment number increases. Therefore, the MCAF method cannot be applied in LTA. It should be noted that the accumulated SNR of two data segments of DATA2 is much higher than that of the one data segment. This phenomenon can also be observed from Table 2 below, where the estimated values of FDOA parameters are similar for the first two segments of DATA2, and the energy of the two segments can be concentrated.

Table 1
The Accumulated SNRs of Signals With Different Accumulation Time

Accumulation time (in segment)	DATA1 SNR (dB)	DATA2 SNR (dB)
1 segment	33.4811	26.0059
2 segments	31.5173	36.5699
3 segments	31.0811	34.7828
4 segments	30.0816	33.6366
5 segments	29.0821	32.6238
6 segments	28.2864	31.9216
7 segments	27.6641	31.2738
8 segments	27.3136	30.6425
9 segments	26.8386	30.1458
10 segments	26.3160	29.7737
11 segments	26.1602	29.6111
12 segments	25.8261	29.2125
13 segments	26.2189	28.6473
14 segments	–	28.2775

4.2. Results of FDOA Compensation Inside the Segment

After dividing the test data into short signal segments, the proposed LTA method is used to estimate the three parameters, that is, the TDOA, the initial FDOA, and the FDOA variation rate for each segment. The estimated parameters are listed in Table 2. In this experiment, to evaluate the performance of energy concentration, the FDOA compensation is used to compensate the FDOA variation in each segment.

Figure 9 shows the estimated FDOAs without compensation, while the FDOAs after compensation are shown in Figure 10. It is seen that the FDOA curve with compensation is smoother than that without compensation, which indicates that the energy of the segment is concentrated and the accuracy of the estimated FDOA is improved.

The energy concentration after FDOA compensation is also verified in Figure 11, which compares the spectrum of the first segment without compensation and that with compensation. After compensating the FDOA variation inside the segment, the bandwidth of the signal is reducing, and the accumulated SNR is increasing. Table 3 lists the accumulated SNRs of all the segments with and without FDOA compensation. By using the proposed

Table 2
The Values of the Three Parameters Estimated by the Proposed Method

Segment	DATA1 $\frac{\hat{D}_i}{f_s}$ (s)	DATA1 $\Delta\hat{f}_i$ (Hz)	DATA1 $\hat{k}_i$ (Hz/s)	DATA2 $\frac{\hat{D}_i}{f_s}$ (s)	DATA2 $\Delta\hat{f}_i$ (Hz)	DATA2 $\hat{k}_i$ (Hz/s)
1	0.00733568	−992.5827	−0.01456937	0.00750856	−459.5441	−0.01768565
2	0.00733608	−991.975	−0.01665916	0.00750856	−459.0044	−0.01698031
3	0.00733648	−991.3533	−0.01529526	0.00750864	−458.2544	−0.0145953
4	0.00733688	−990.6035	−0.01035645	0.00750872	−458.0043	−0.01943801
5	0.00733728	−990.106	−0.01302044	0.00750872	−457.3312	−0.01829269
6	0.00733768	−989.5614	−0.014962	0.0075088	−456.6051	−0.01964856
7	0.00733808	−989.0306	−0.01934972	0.00750888	−456.1456	−0.01785793
8	0.00733848	−988.1296	−0.01166052	0.00750888	−455.4707	−0.01897021
9	0.00733888	−987.6173	−0.01684549	0.00750896	−454.6938	−0.01809856
10	0.00733928	−987.0038	−0.01485022	0.00750896	−453.9046	−0.01819516
11	0.00733968	−986.2387	−0.01397045	0.00750904	−453.2467	−0.01901505
12	0.00734008	−985.629	−0.0105904	0.00750912	−452.5214	−0.01468732
13	0.00734048	−985.0543	−0.01005625	0.00750912	−452.0092	−0.01975291
14				0.0075092	−451.2957	−0.01727597

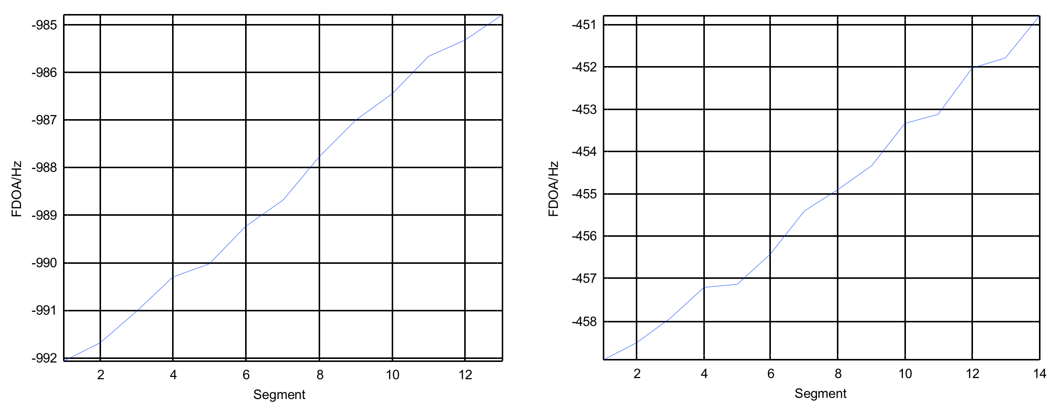

(a) (b)

Figure 9. Estimated FDOAs for all the segments without FDOA compensation. (a) Estimated FDOAs of DATA1. (b) Estimated FDOAs of DATA2.

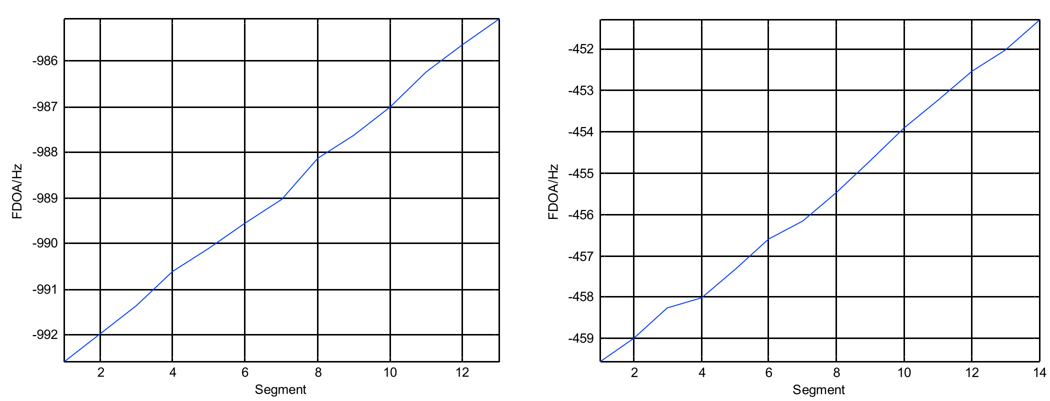

(a) (b)

Figure 10. Estimated FDOAs for all the segments with FDOA compensation. (a) Estimated FDOAs of DATA1. (b) Estimated FDOAs of DATA2.

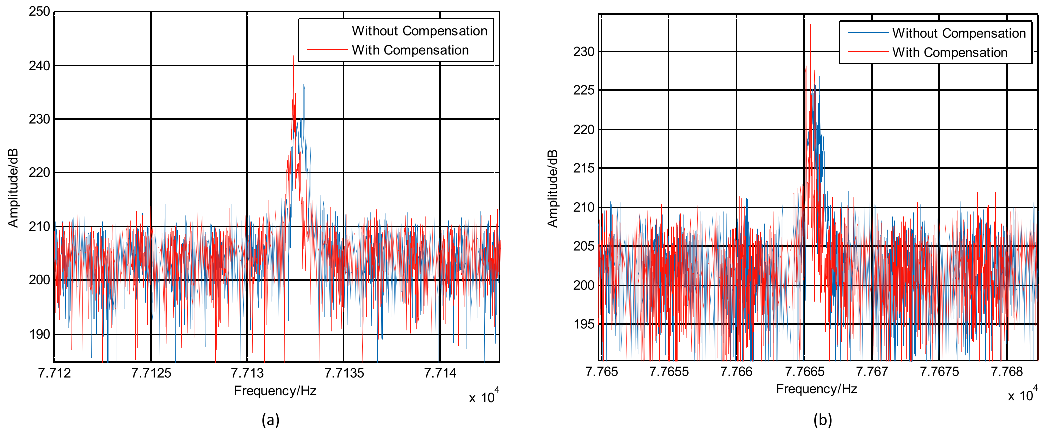

Figure 11. Spectrum comparison between the first segment without compensation and that with compensation. (a) The spectrums of the first segment of DATA1. (b) The spectrums of the first segment of DATA2.

Table 3
The SNR Values of All the Segments Without Compensation and That With Compensation

Segment	DATA1 Original SNR (dB)	DATA1 Compensated SNR (dB)	DATA2 Original SNR (dB)	DATA2 Compensated SNR (dB)
1	33.4811	38.8128	26.0059	32.5638
2	32.8332	37.2196	26.5139	30.855
3	33.008	37.5895	28.8384	32.2465
4	35.3408	38.6773	26.8717	30.5025
5	34.5743	39.9859	27.9548	29.5295
6	32.5057	40.3648	28.2144	32.498
7	34.2748	37.2553	25.7832	30.8524
8	32.7221	38.6302	25.4665	31.2759
9	33.0705	36.0348	25.319	29.8058
10	31.3774	39.7855	25.8876	32.2983
11	33.5222	37.1157	27.1349	32.5914
12	32.7898	34.5909	26.8582	35.4491
13	36.1084	36.4489	26.3036	30.4998
14			27.4167	33.2576
Average	33.5083	37.8855	26.7549	31.7304

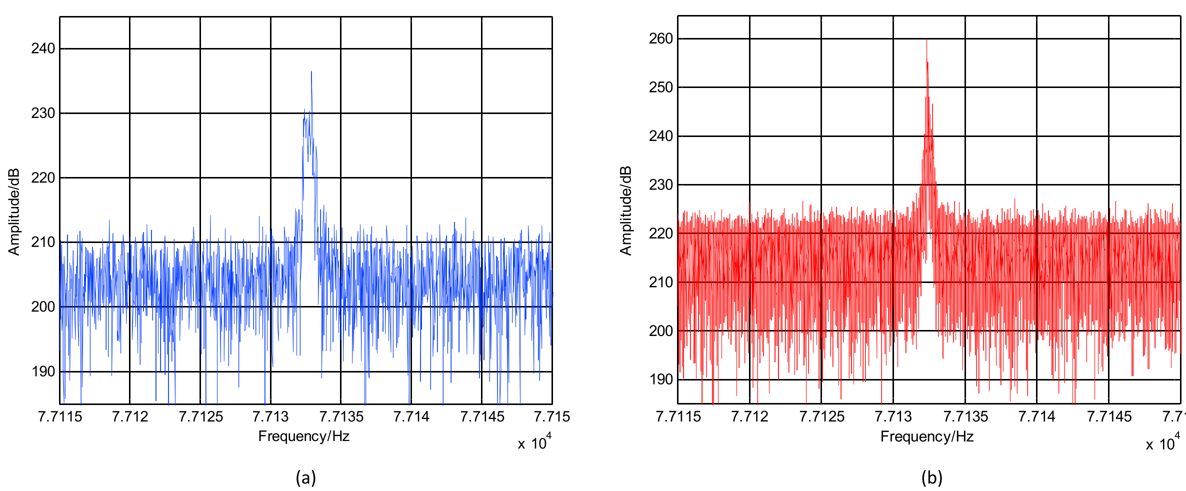

Figure 12. The accumulation result of DATA1. (a) The spectrum of the first segment without compensation. (b) The spectrum of the spliced signal (including all the 13 segments).

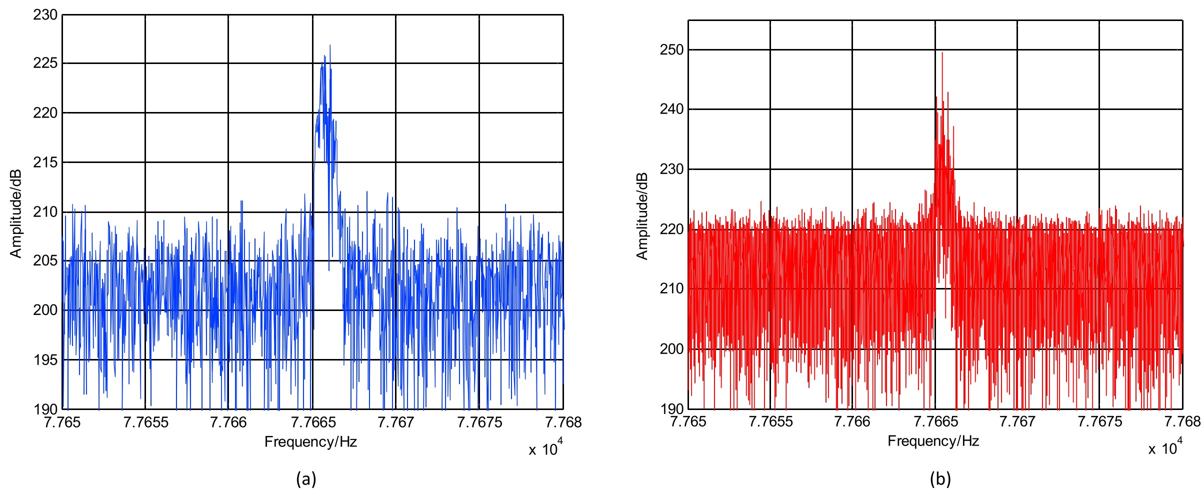

Figure 13. The accumulation result of DATA2. (a) The spectrum of the first segment without compensation. (b) The spectrum of the spliced signal (including all the 14 segments).

LTA method, an average SNR gain of 4.3772 dB is achieved for each segment of DATA1, and an average gain of 4.9755 dB is achieved for each segment of DATA2.

4.3. Results of FDOA Compensation for LTA

In this experiment, to demonstrate the effectiveness of the proposed method in LTA, we not only compensate the FDOA variation $\hat{k}_i$ inside the segment but also compensate the FDOA difference $(\Delta\hat{f}_i - \Delta\hat{f}_1)$ for each segment. In other words, the FDOAs of all the segments are aligned with the FDOA of the first segment, that is, $\Delta\hat{f}_1$. After the above operation, the correlation results of all the segments are spliced again. Figure 12a shows the spectrum of the first segment of DATA1 without compensation, and Figure 12b shows the spectrum of the spliced signal of DATA1 after compensation. The results of DATA2 are shown in Figure 13. By comparing the spectrums, it is seen that the amplitude of the spliced signal after compensation is much higher than that of the first segment without compensation. Besides, although the time length of the spliced signal is much larger than the first segment, the bandwidth of the spliced signal becomes narrower. This shows that the FDOA variation has been compensated in the accumulation time.

For DATA1, the average accumulated SNR of a segment with compensation is 37.8855 dB, while the accumulated SNR of all the 13 segments with compensation is 45.8326 dB. For DATA2, the two SNR values are 31.7304 dB and 37.0792 dB. Compared to a single segment, the SNR gains achieved by accumulating all the segments are 7.9471 dB and 5.3488 dB for DATA1 and DATA2, respectively. Moreover, from Table 1, it is found that the accumulated SNR of all the segments without compensation is 26.2189 dB for DATA1, and 28.2775 dB for DATA2. The total SNR gains of the two test data achieved by the proposed method are 19.6137 dB and 8.8017 dB, respectively. From Table 1, it is noted that the correlation of the estimated parameters between different segments are higher in DATA2 than in DATA1; thus, the SNR gain of DATA2 is less than that of DATA1. When the number of segments increases, the SNR gain will also increase. Therefore, the proposed LTA method can be applied to the signals with arbitrary time length.

5. Conclusion

TDOA/FDOA estimation plays an important role in double-satellite localization system. The LTA method can be used to concentrate the signal energy and improve the accuracy of the estimated parameters, especially for the low SNR cases. However, the traditional CAF-based method assumes that the TDOA/FDOA of the two received signals is constant, which does not hold in LTA cases. To solve this problem, a novel LTA method based on signal segmentation is proposed in this paper. In the proposed method, the two input signals are divided into short signal segments. The length of the segment is determined by a principle that the TDOA variation would not exceed a sampling period. Thus, the TDOA of each segment can be considered as constant. For each segment, the MCAF-SOS algorithm is performed to estimate the TDOA firstly, then the Rife iterative algorithm and the SQP algorithm are carried out to estimate the FDOA and the FDOA variation rate, respectively. After compensating the FDOA difference between the signal segments, the correlation results are spliced again to form a complete signal without FDOA variation. As a result, after FDOA compensation and FFT operation, the signal energy is concentrated and a significant SNR gain is achieved. In addition, the proposed LTA method can be applied to any received signals with arbitrary time length. Experimental results on real data verify the effectiveness of the proposed LTA method.

Acknowledgments
The research was supported by the Science and Technique Commission Foundation of Fujian Province, China (grant 2018H61010043), the Principal Foundation of Xiamen University, the Open-End Fund of BITTT Key Laboratory of Space Object Measurement, and the National Natural Science Foundation of China (grant 62101196). The simulation data set was deposited in Baidu Netdisk https://pan.baidu.com/s/1hr81PEc, and readers can use the data set to reproduce the proposed LTA method.

References

Belanger, S. P. (1993). Multipath TDOA and FDOA estimation using the EM algorithm. *1993 IEEE International Conference on Acoustics, Speech, Signal Process*, *4*, 168–171.
Coleman, M. (2015). Technology and thinking to combat satellite interference. In *Milsatcoms* (pp. 1–35). London, UK.
Dandawate, A. V., & Giannakis, G. B. (1993). Differential delay-Doppler estimation using second- and higher-order ambiguity functions. *IEEE Xplore: IEE Proceedings F - Radar and Signal Processing*, *140*, 410–418.
Dempster, A. G. (2006). Dilution of precision in angle-of-arrival positioning systems. *Electronics Letters*, *42*, 291–292.
Dempster, A. G., & Cetin, E. (2016). Interference localization for satellite navigation systems. *Proceedings of the IEEE*, *104*, 1–9.
Dempster, A. P., Laird, N. M., & Rubin, D. B. (1977). Maximum likelihood from incomplete data via the EM algorithm. *Elearn*, *39*, 1–38.
Deng, B., Xiong, J. Y, & Xia, C. X. (2012). The observability analysis of aerial moving target location based on dual-satellite geolocation system. In *2012 International Conference on Computer Science and Information Processing* (pp. 12–15).
Fowler, M. L, & Hu, X. (2008). Signal models for TDOA/FDOA estimation. *IEEE Transactions on Aerospace and Electronic Systems*, *4*, 1543–1550.
Guo, F. Y., Zhang, Z. J, & Yang, L. S. (2016). TDOA/FDOA estimation method based on dechirp. *IET Signal Process*, *10*, 186–492.
Haworth, D. P. (2000). Locating the source of an unknown signal. US. Patent 6,018,312.
Haworth, D. P., Smith, N. G., Bardelli, R., & Clement, T. (1997). Interference localization for EUTELSAT satellites the first European transmitter location system. *International Journal of Satellite Communications and Networking*, *15*, 155–183.
Ho, D. K. C., Chu, J. C., & Downey, M. L. (2013). Determining transmit location of an emitter using a single geostationary satellite. US. Patent 8,462,044.
Ho, K. C., & Xu, W. W. (2004). An accurate algebraic solution for moving source location using TDOA and FDOA measurements. *IEEE Transactions on Signal Processing*, *52*, 2453–2463.
Hu, D. X., Huang, Z., Liang, K. Q., & Zhang, S. Y. (2016). Coherent TDOA/FDOA estimation method for frequency-hopping signal. In *2016 8th International Conference on Wireless Communications & Signal Processing* (pp. 1–5).
Isoz, O., Buehler, S. A., Kinch, K., Bonnedal, M., & Akos, D. M. (2014). Interference from terrestrial sources and its impact on the GRAS GPS radio occultation receiver. *Radio Science*, *49*, 1–6. https://doi.org/10.1002/2013RS005243
Kalantari, A., Maleki, S., Chatzinotas, S., & Ottersten, B. (2016). Frequency of arrival-based interference localization using a single satellite. In *2016 8th Advanced Satellite Multimedia Systems Conference and the 14th Signal Processing for Space Communications Workshop (ASMS/SPSC)* (pp. 1–6).
Kallan, Y., & Baykal, B. (2014). Frequency-based target localization methods for widely separated MIMO radar. *Radio Science*, *49*, 53–67. https://doi.org/10.1002/2013RS005245
Kay, S. M. (1993). *Fundamentals of statistical signal processing: Estimation theory*. Englewood Cliffs, NJ: Prentice Hall.
Kimball, S. F. (2011). Method and apparatus for locating the source of radio frequency emissions. US. Patent, 7,916,085,29.
Knapp, C., & Carter, G. (1977). Time delay estimation in the presence of relative motion. *ICASSP '77. IEEE International Conference on Acoustics, Speech and Signal Processing*, *2*, 280–283.
Lin, D. M., & Tsui, J. B. Y. (2002). A weak signal tracking technique for a stand-alone software GPS receiver. In *Proceedings of International Technical Meeting of the Satellite Division of The Institute of Navigation* (pp. 2534–2538). Portland, OR.
Lin, D. M., & Tsui, J. B. Y. (2014). One intelligent algorithm for estimation of TDOA and FDOA. In *2014 IEEE 7th Joint International Information Technology and Artificial Intelligence Conference* (pp. 492–496).
Malaney, R. A. (2007). Nuisance parameters and location accuracy in log-normal fading models. *IEEE Transactions on Wireless Communications*, *6*, 937–947.
Mason, J. (2004). Algebraic two-satellite TOA/FOA position solution on an ellipsoidal earth. *IEEE Transactions on Aerospace and Electronic Systems*, *40*, 1087–1092.
Michael, N. (2015). Method for identifying interfering transmitters from a plurality of known satellite transmitters. *Patent WO 2015062810 A1*.
Musicki, D., & Koch, W. (2008). Geolocaion using TDOA and FDOA measurements. In *2008 11th International Conference on Information Fusion* (pp. 1–8).
Musicki, D., Kaune, R., & Koch, W. (2010). Mobile emitter geolocation and tracking using TDOA and FDOA measurements. *IEEE Transactions on Signal Processing*, *58*, 1863–1874.
Rife, D. C, & Vincent, G. A. (1970). Use of the discrete Fourier transform in the measurement of frequencies and levels of tones. *Bell System Technical Journal*, *49*, 197–228.
Shan, T., Tao, R., & Sun, R. R. (2008). Fourth-order ambiguity function based on the fractional Fourier transform. *2008 Congress on Image and Signal Processing*, *5*, 447–451.
Shin, D. C., & Nikias, C. L. (1993). Complex ambiguity function based on fourth-order statistics for joint estimation of frequency-delay and time-delay of arrival. *Asilomar Conference on Signals, Systems, and Computers*, *1*, 461–465.
Smith, W. W. J., & Steffes, P. G. (1990). A satellite interference location system using differential time and phase measurement techniques. In *International Carnahan Conference on Security Technology: Crime Countermeasures* (pp. 38–41).
Spellucci, P. (1998). An SQP method for general nonlinear programs using only equality constrained subproblems. *Programs in Mathematics*, *82*, 413–448.
Stein, S. (1993). Differential delay/Doppler ML estimation with unknown signals. *IEEE Transactions on Signal Processing*, *41*, 2717–2719.
Stein, S. (1981). Algorithms for ambiguity function processing. *IEEE Transactions on Acoustics*, *29*, 588–599.
Thompson, R. J. R. (2015). Detection and localisation of radio frequency interference to GNSS reference stations (PhD Dissertation), Sydney, Australia.
Trinkle, M., & Gray, D. A. (2002). Interference localization trials using adaptive antenna arrays. In *Proceedings of the 16th International Technical Meeting of the Satellite Division of The Institute of Navigation (ION GPS 2002)* (pp. 613–619).
Tsui, B. Y. (2004). *Digital techniques for wideband receivers* (2nd ed.). Raleigh, NC: SciTech Publishing.
Tsui, J. B. Y. (2005). *Fundamentals of Global Positioning System receivers: A software approach* (2nd ed., pp. 93–99). Hoboken, NJ: Wiley & Sons.
Wax, M. (1982). The joint estimation of differential delay, Doppler, and phase. *IEEE Transactions on Information Theory*, *28*, 817–820.

Wu, S. L., Luo, J. Q., & Gong, L. L. (2010). Joint FDOA and TDOA location algorithm and performance analysis of dual-satellite formations. *2010 2nd International Conference on Signal Processing Systems*, *2*, 339–342.

Xiao, Y. C., Wei, P., Xiao, X. C., & Tai, H. M. (2004). Fast and accurate single frequency estimator. *Electronics Letters*, *40*, 910–911.

Xu, Z., Trinkle, M., & Gray, D. A. (2010). A modelled eigenstructure based antenna array calibration algorithm for GPS. In *Proceeding of 23rd International Technical Meeting of The Satellite Division of the Institute of Navigation* (pp. 3220–3228).

Yao, G. X., Liu, Z. W., & Xu, Y. G. (2005). TDOA/FDOA joint estimation in a correlated noise environment. *2005 IEEE International Symposium on Microwave, Antenna, Propagation and EMC Technologies for Wireless Communications*, *1*, 831–834.

Youn, D. H., & Ahmed, N. (1984). Comparison of two adaptive methods for time delay estimation. *IEEE International Conference on Acoustics, Speech and Signal Processing*, *5*, 617.

Zhang, W., & Zhang, G. X. (2011). An efficient algorithm for TDOA/FDOA estimation based on approximate coherent accumulative of short-time CAF. In *2011 International Conference on Wireless Communications and Signal Processing* (pp. 1–4).